Supplementary Methods

Gene silencing and oncogenic function assays

shRNAs were transfected with psPAX2 packaging and pMD2.G envelope plasmid to HEK293FT cells for 2 days using Lipofectamine 3000 (ThermoFisher Scientific). Thereafter, PC cells were infected with viral supernatants in the presence of 8 μg/ml polybrene. Stable cells were generated using puromycin selection. A list of shRNAs and constructs is provided in Table S2. Efficiency of knockdown and overexpression was verified by quantitative PCR (qPCR) and Western blot. Cells were treated with shRNAs or inhibitors. After stably knocking down CSN5 in PC cells, cell viability was assessed using CellTiter-Glo luminescent cell viability assay (Promega). Apoptosis was detected using the Muse Cell Cycle Kit and the Muse Annexin V & Dead Cell Kit (MilliporeSigma). DNA damage was detected at 24 hours after treatment of inhibitors in cells by using Muse Multi-Color DNA Damage Kit (MilliporeSigma).

Soft agar assays and invasion assays

Soft agar assays were performed in 6-well tissue culture plates by placing cells (2-5 x 10^4/well) in 2 ml of 0.3% soft-agar above a 2-ml layer of 0.5% agar. After two weeks' incubation, cells were stained with 1 mg/ml MTT in medium for 1 hour. Colonies were detected and counted using GelCount technology (Oxford Optronix Ltd., Oxford, UK). Invasion assays were performed in a Matrigel invasion chamber (Fisher Scientific) with cells in the top chamber in serum-free media, while 10% FBS in the lower chamber was used as a chemo-attractant. After indicated times, cells in the bottom chamber were fixed in methanol and stained with crystal violet, photographed, and counted under phase-contrast microscopy.

CUT&Tag analysis, DNA sequencing, and data analysis

Cells (1-2x10^6) were harvested and washed with Wash Buffer, then 10 µl of activated concanavalin A coated magnetic beads (Bangs Laboratories) were added and incubated at room temperature for 15 min. After removing the unbound supernatant, bead-bound cells were resuspended in 100 µl DIG Wash Buffer containing 2 mM EDTA and a 1:50 dilution of the appropriate primary antibodies. Three primary antibodies (CSN5: sc-13157; GTX70207; ab124720) incubation were performed on a rotating platform for 2 h at room temperature. The primary antibodies were removed and secondary antibodies were added and incubated at room temperature for 30 min. Unbound antibodies were removed by washing with DIG Wash Buffer. pA-Tn5 adapter complex that was diluted 200x in Dig-med Buffer was incubated with cells at room temperature for 1 h. Unbound pA-Tn5 protein was removed with Dig-med Buffer wash. Resuspended cells in tagmentation buffer (10 mM MgCl2 in Dig-med Buffer) was incubated at 37 °C for 1 h. Buffer PB from the MinElute PCR Purification Kit (Qiagen) was used to stop the tagmentation. The same kit was used to extract DNA by following the manufacturer's instruction. To amplify libraries, DNA was mixed with i5 and i7 primers and NEBNext High-Fidelity 2X PCR Master Mix and amplified by following cycling conditions: 72 °C for 5 min (gap filling); 98 °C for 30 s; 14 cycles of 98 °C for 10 s and 63 °C for 30 s; final extension at 72 °C for 1 min and hold at 8 °C. For post-PCR clean-up, 1.1× volume of Ampure XP beads (Beckman Coulter) were added and incubated for 15 min at room temperature, washed in 80% ethanol, and eluted in 10 mM Tris pH 8.0.

After DNA quantification and quality control with PicoGreen on an Agilent Bioanalyzer, the CUT&Tag DNA libraries were pooled equimolar and run on a NovaSeq 6000 in a PE50 run, using the NovaSeq 6000 S1 Reagent Kit (100 Cycles) (Illumina). The loading concentration was

0.9nM and a 1% spike-in of PhiX was added to the run to increase diversity and for quality control purposes. The run yielded on average 79M reads per sample.

CUT&Tag sequencing reads were trimmed and filtered for quality and adapter content using version 0.4.5 of Trim Galore! (https://www.bioinformatics.babraham.ac.uk/projects/trim_galore) with a quality setting of 15, and running version 1.15 of Cutadapt and version 0.11.5 of FastQC. Reads were aligned to human assembly hg19 with version 2.3.4.1 of Bowtie 2 (http://bowtie-bio.sourceforge.net/bowtie2/index.shtml) and were de-duplicated using MarkDuplicates in version 2.16.0 of Picard Tools (Broad Institute). To ascertain regions of enrichment, MACS2 (https://github.com/taoliu/MACS) was used with a p-value setting of 0.001. The BEDTools suite (http://bedtools.readthedocs.io) was used to create normalized read density profiles. A global peak atlas was created by first removing blacklisted regions (http://mitra.stanford.edu/kundaje/akundaje/release/blacklists/hg19-human/hg19.blacklist.bed.gz) then merging all peaks within 500 bp and counting reads with version 1.6.1 of featureCounts (http://subread.sourceforge.net). For samples without replicates, differential peaks were calculated using MACS2 treatment and control parameters and swapping the two conditions. Peak-gene associations were created by assigning peaks to genes using linear genomic distance to transcription start site. Peak intersections were calculated using bedtools v2.29.1 and intersectBed with 1 bp overlap. Gene set enrichment analysis (GSEA; http://software.broadinstitute.org/gsea) was performed with the pre-ranked option and default parameters, where each gene was assigned the single peak with the largest (in magnitude) log2 fold change associated with it. Composite and tornado plots were created with deepTools v3.3.0 by running computeMatrix and plotHeatmap on normalized bigwigs by averaging over 25 bp windows and flanking region defined by the surrounding 2 kb from the peak center. Motif signatures were obtained using HOMER (hypergeometric optimization of motif enrichment) v4.5 (http://homer.ucsd.edu).

Figure S1

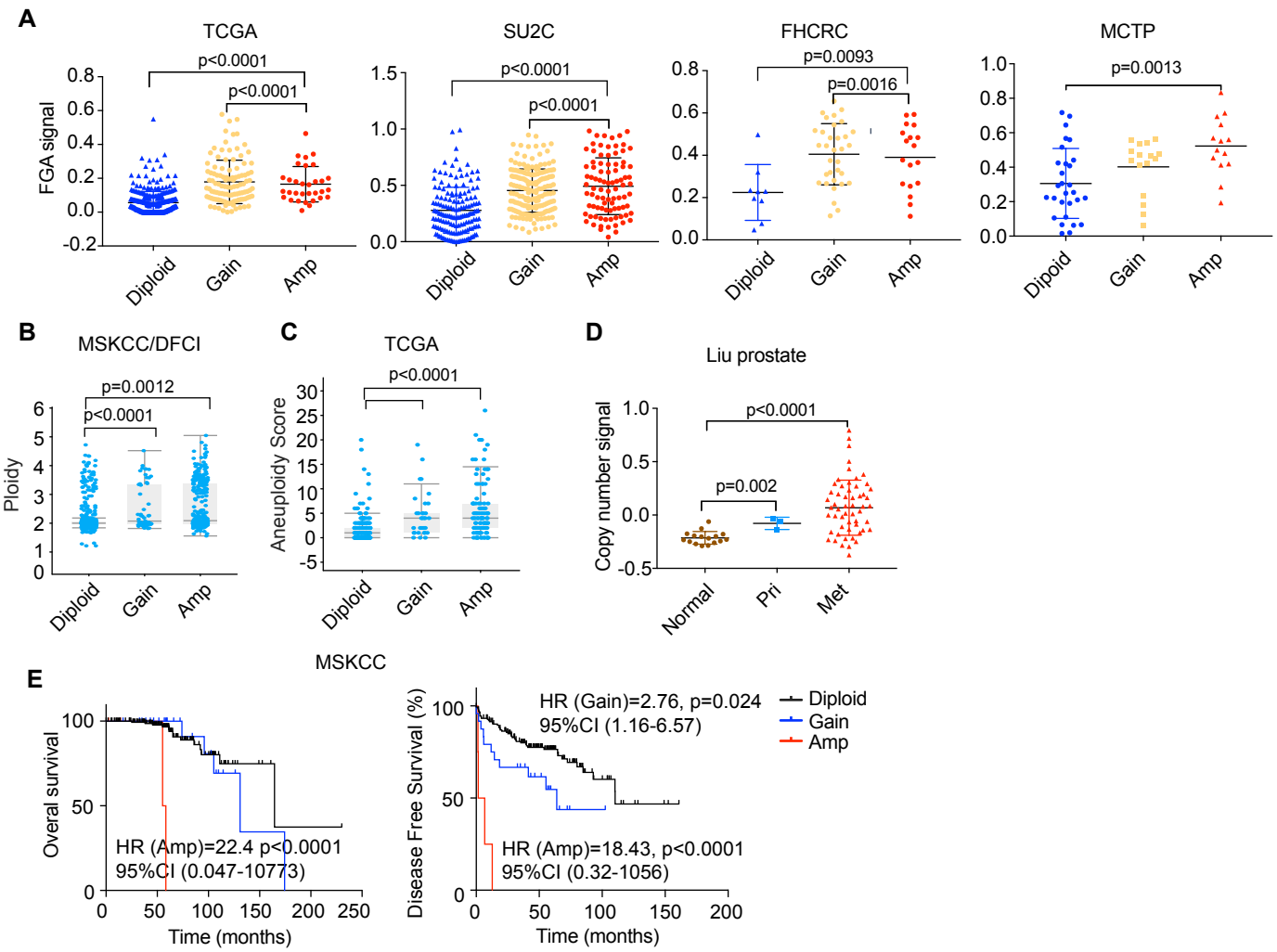
A
TCGA
SU2C
FHCRC
MCTP
FGA signal
p<0.0001
p<0.0001
p<0.0001
p<0.0001
p=0.0093
p=0.0016
p=0.0013
Diploid
Gain
Amp
Dipoid
B
MSKCC/DFCI
Ploidy
p=0.0012
p<0.0001
C
TCGA
Aneuploidy Score
p<0.0001
D
Liu prostate
Copy number signal
p<0.0001
p=0.002
Normal
Pri
Met
E
MSKCC
Overal survival
HR (Amp)=22.4 p<0.0001
95%CI (0.047-10773)
Time (months)
Disease Free Survival (%)
HR (Gain)=2.76, p=0.024
95%CI (1.16-6.57)
HR (Amp)=18.43, p<0.0001
95%CI (0.32-1056)
Diploid
Gain
Amp

Figure S2

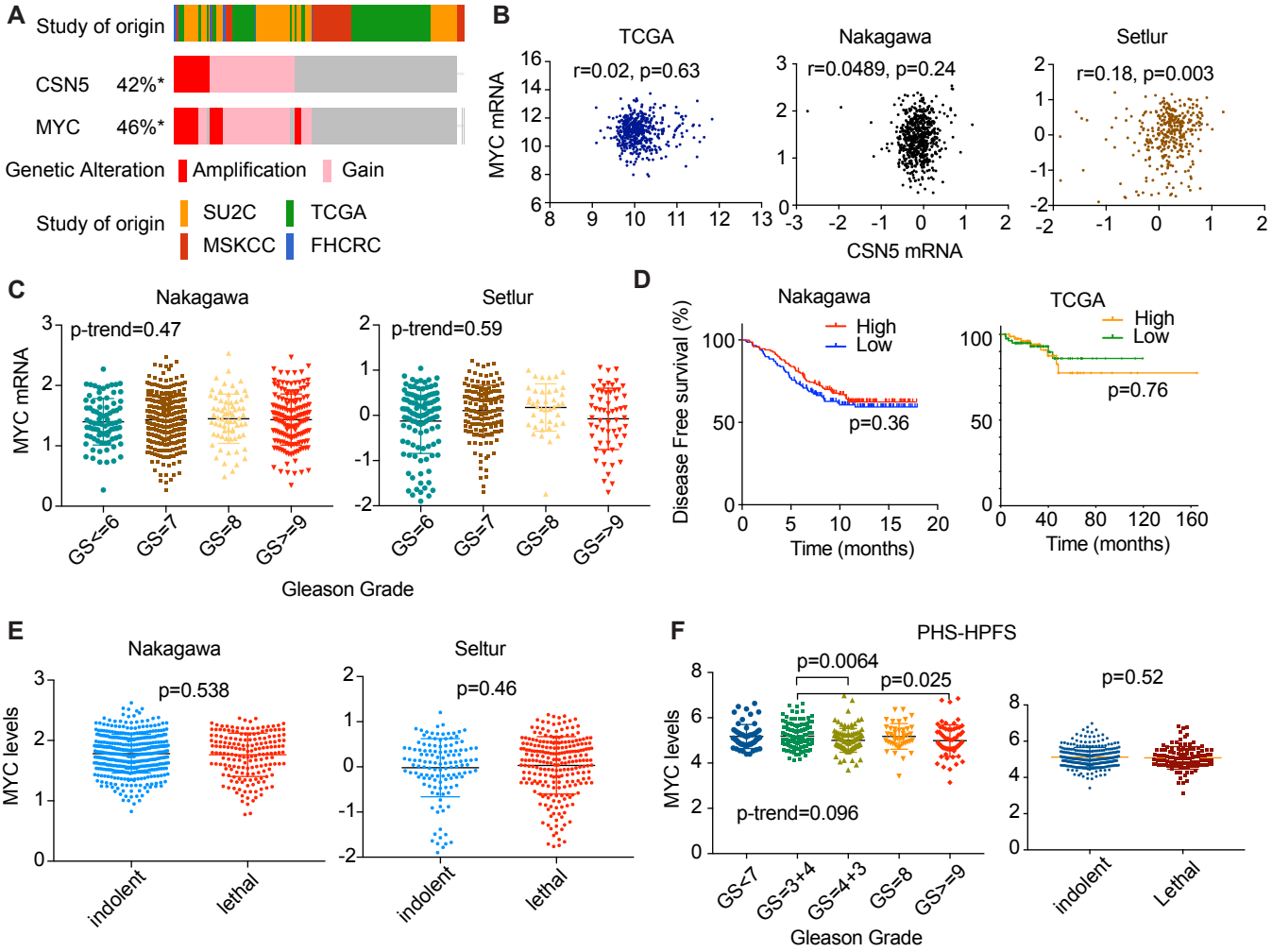
A
Study of origin
CSN5 42%*
MYC 46%*
Genetic Alteration
Amplification
Gain
Study of origin
SU2C
TCGA
MSKCC
FHCRC
B
TCGA
r=0.02, p=0.63
Nakagawa
r=0.0489, p=0.24
Setlur
r=0.18, p=0.003
MYC mRNA
CSN5 mRNA
C
Nakagawa
p-trend=0.47
Setlur
p-trend=0.59
MYC mRNA
GS<=6
GS=7
GS=8
GS>=9
Gleason Grade
D
Nakagawa
High
Low
p=0.36
TCGA
p=0.76
Disease Free survival (%)
Time (months)
E
Nakagawa
p=0.538
Seltur
p=0.46
MYC levels
indolent
lethal
F
PHS-HPFS
p=0.0064
p=0.025
p-trend=0.096
p=0.52
MYC levels
GS<7
GS=3+4
GS=4+3
GS=8
GS>=9
Gleason Grade
indolent
Lethal

Figure S3

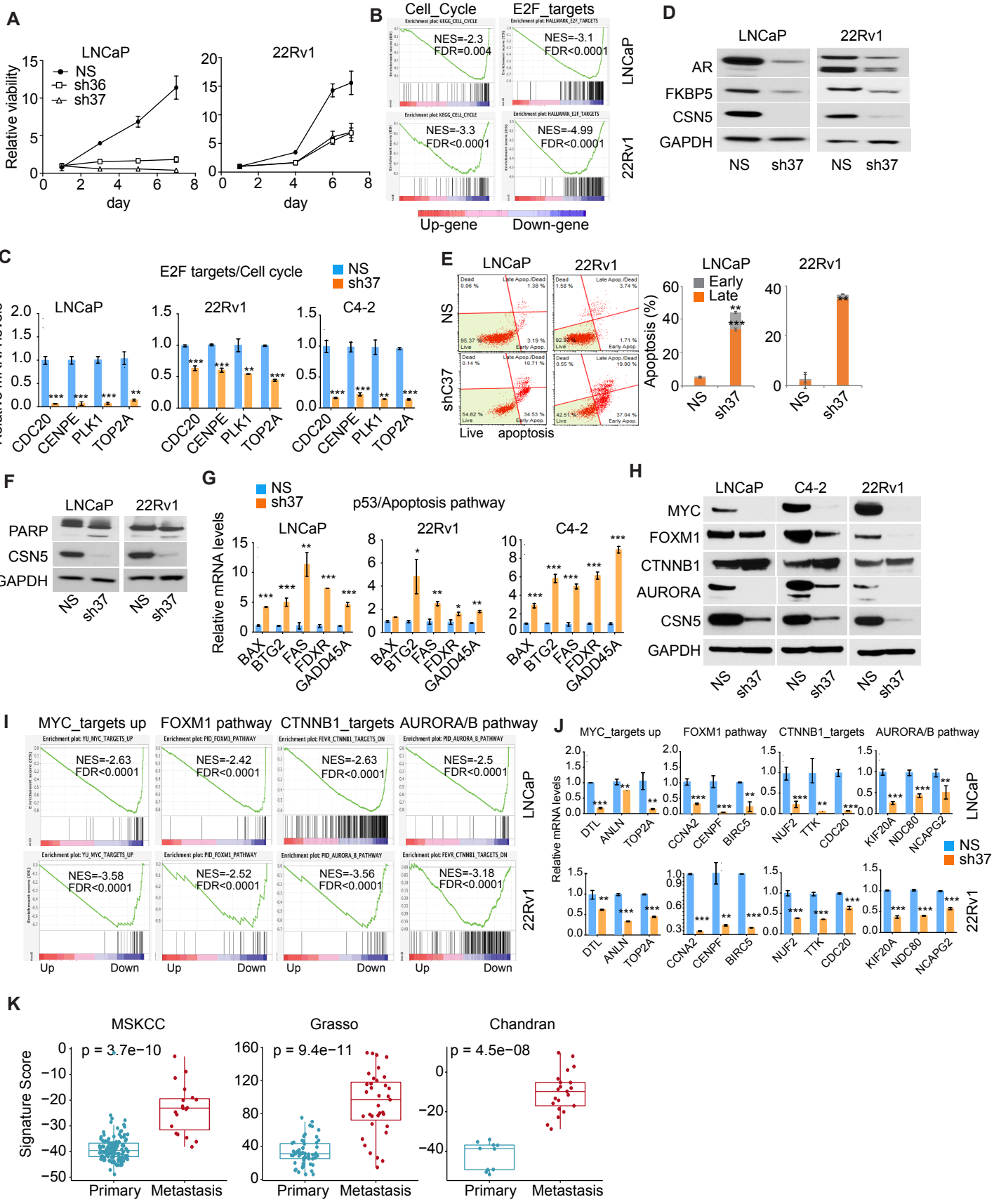
A
LNCaP
22Rv1
NS
sh36
sh37
Relative viability
day
B
Cell_Cycle
E2F_targets
NES=-2.3
FDR=0.004
NES=-3.1
FDR<0.0001
NES=-3.3
FDR<0.0001
NES=-4.99
FDR<0.0001
LNCaP
22Rv1
Up-gene
Down-gene
D
LNCaP
22Rv1
AR
FKBP5
CSN5
GAPDH
NS
sh37
C
E2F targets/Cell cycle
NS
sh37
Relative mRNA levels
CDC20
CENPE
PLK1
TOP2A
C4-2
E
LNCaP
22Rv1
NS
shC37
Live
apoptosis
Early
Late
Apoptosis (%)
F
PARP
CSN5
GAPDH
G
p53/Apoptosis pathway
BAX
BTG2
FAS
FDXR
GADD45A
H
MYC
FOXM1
CTNNB1
AURORA
C4-2
I
MYC_targets up
FOXM1 pathway
CTNNB1_targets
AURORA/B pathway
NES=-2.63
FDR<0.0001
NES=-2.42
FDR<0.0001
NES=-2.63
FDR<0.0001
NES=-2.5
FDR<0.0001
NES=-3.58
FDR<0.0001
NES=-2.52
FDR<0.0001
NES=-3.56
FDR<0.0001
NES=-3.18
FDR<0.0001
Up
Down
J
DTL
ANLN
TOP2A
CCNA2
CENPF
BIRC5
NUF2
TTK
CDC20
KIF20A
NDC80
NCAPG2
K
MSKCC
Grasso
Chandran
p = 3.7e−10
p = 9.4e−11
p = 4.5e−08
Signature Score
Primary
Metastasis

Figure S4

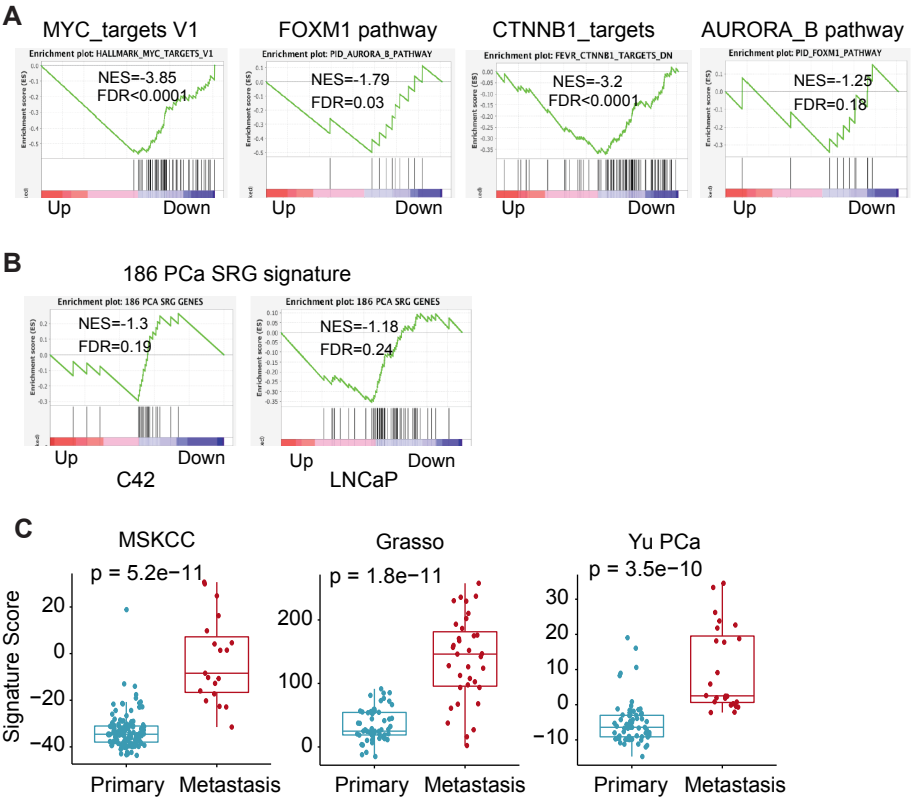
A
MYC_targets V1
NES=-3.85
FDR<0.0001
Up
Down
FOXM1 pathway
NES=-1.79
FDR=0.03
Up
Down
CTNNB1_targets
NES=-3.2
FDR<0.0001
Up
Down
AURORA_B pathway
NES=-1.25
FDR=0.18
Up
Down
B
186 PCa SRG signature
NES=-1.3
FDR=0.19
Up
Down
C42
NES=-1.18
FDR=0.24
Up
Down
LNCaP
C
MSKCC
p = 5.2e−11
Grasso
p = 1.8e−11
Yu PCa
p = 3.5e−10
Signature Score
Primary
Metastasis
Primary
Metastasis
Primary
Metastasis

Figure S5

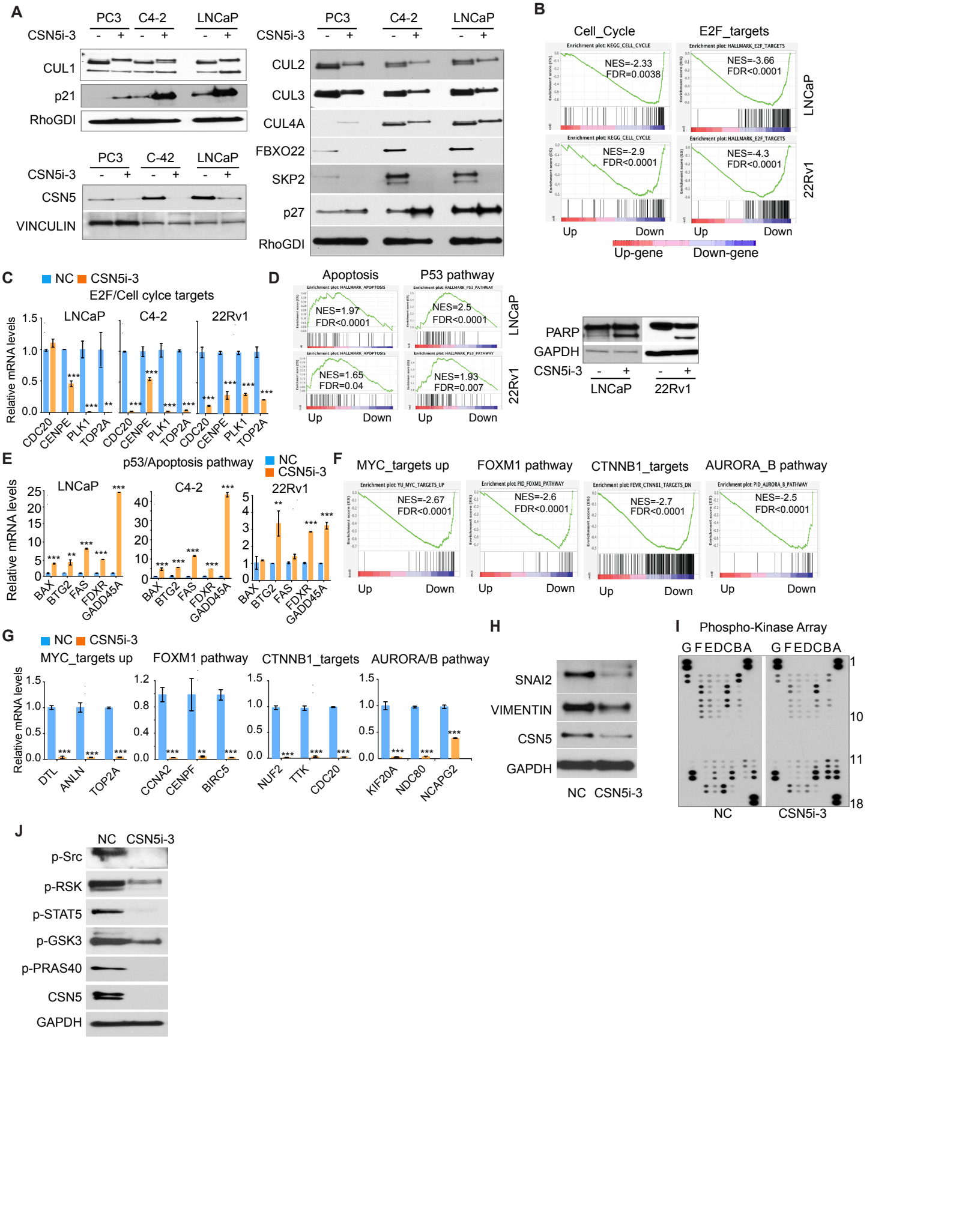
A
PC3
C4-2
LNCaP
CSN5i-3
CUL1
p21
RhoGDI
CUL2
CUL3
CUL4A
FBXO22
SKP2
p27
C-42
CSN5
VINCULIN
B
Cell_Cycle
E2F_targets
NES=-2.33
FDR=0.0038
NES=-3.66
FDR<0.0001
NES=-2.9
FDR<0.0001
NES=-4.3
FDR<0.0001
LNCaP
22Rv1
Up
Down
Up-gene
Down-gene
C
NC
CSN5i-3
E2F/Cell cylce targets
Relative mRNA levels
CDC20
CENPE
PLK1
TOP2A
D
Apoptosis
P53 pathway
NES=1.97
FDR<0.0001
NES=2.5
FDR<0.0001
NES=1.65
FDR=0.04
NES=1.93
FDR=0.007
PARP
GAPDH
E
p53/Apoptosis pathway
BAX
BTG2
FAS
FDXR
GADD45A
F
MYC_targets up
FOXM1 pathway
CTNNB1_targets
AURORA_B pathway
NES=-2.67
FDR<0.0001
NES=-2.6
FDR<0.0001
NES=-2.7
FDR<0.0001
NES=-2.5
FDR<0.0001
G
MYC_targets up
FOXM1 pathway
CTNNB1_targets
AURORA/B pathway
DTL
ANLN
TOP2A
CCNA2
CENPF
BIRC5
NUF2
TTK
CDC20
KIF20A
NDC80
NCAPG2
H
SNAI2
VIMENTIN
CSN5
GAPDH
I
Phospho-Kinase Array
G F E D C B A
J
p-Src
p-RSK
p-STAT5
p-GSK3
p-PRAS40
CSN5
GAPDH

Figure S6

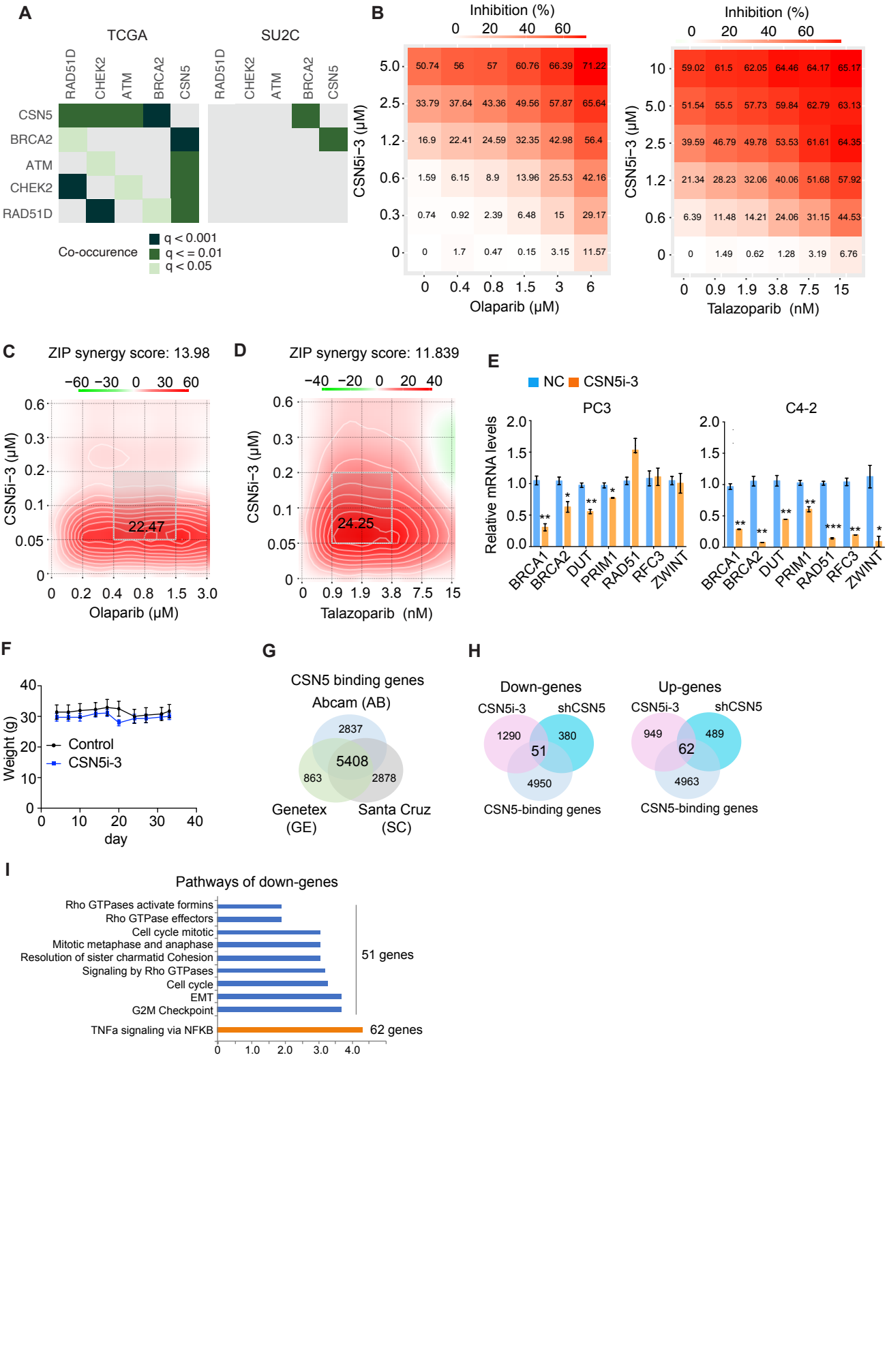
A
TCGA
SU2C
RAD51D
CHEK2
ATM
BRCA2
CSN5
Co-occurence
q < 0.001
q < = 0.01
q < 0.05
B
Inhibition (%)
0 20 40 60
CSN5i−3 (μM)
Olaparib (μM)
Talazoparib (nM)
C
ZIP synergy score: 13.98
22.47
D
ZIP synergy score: 11.839
24.25
E
NC
CSN5i-3
PC3
C4-2
Relative mRNA levels
BRCA1
BRCA2
DUT
PRIM1
RAD51
RFC3
ZWINT
F
Weight (g)
Control
CSN5i-3
day
G
CSN5 binding genes
Abcam (AB)
2837
5408
863
2878
Genetex (GE)
Santa Cruz (SC)
H
Down-genes
Up-genes
CSN5i-3
shCSN5
1290
380
51
4950
949
489
62
4963
CSN5-binding genes
I
Pathways of down-genes
Rho GTPases activate formins
Rho GTPase effectors
Cell cycle mitotic
Mitotic metaphase and anaphase
Resolution of sister charmatid Cohesion
Signaling by Rho GTPases
Cell cycle
EMT
G2M Checkpoint
TNFa signaling via NFKB
51 genes
62 genes

Figure S1. Genomic alteration of CSN5 is correlated with poor clinical outcomes in prostate cancer. A, The correlation of CSN5 alteration with fraction genomic altered (FGA) in TCGA, SU2C, FHCRC, and MCTP cohorts. B and C, The correlation of CSN5 alteration with ploidy number (MSKCC/DFCI) (B) and aneuploidy score (TCGA) (C). D, Association of CSN5 alteration with tumor progression in Liu prostate cohort. CSN5 copy number was analyzed in normal, primary (Pri), and metastasis (Met) tissue samples. E, The correlation of CSN5 alteration with overall survival and disease-free survival in MSKCC cohort.

Figure S2. Clinical relevance of CSN5 is independent of MYC in prostate cancer.

A, The genetic alteration of CSN5 and MYC in prostate cancer cohorts. B, The correlation of CSN5 and MYC mRNA levels in three prostate cancer cohorts. C, The correlation of MYC expression with Gleason grade in the Nakagawa and Setlur cohorts. D, The association of MYC expression with disease-free survival in the TCGA and Nakagawa cohorts. E, The correlation of MYC levels with lethality in the Nakagawa and Setlur cohorts. F, The association of MYC expression with Gleason grade and lethality in the combined PHS-HPFS cohort.

Figure S3. Inhibition of CSN5 repressed oncogenic activity of CSN5 in AR positive prostate cancer cells. A, Analysis of cell proliferation in shRNAs infected LNCaP and 22Rv1 cells. Cell proliferation was detected in 7 days. NS, nonspecific shRNA. sh36 and sh37, shRNAs for CSN5. B, Cell cycle and E2F_targets gene sets enrichment in regulated genes by inhibition of CSN5 by sh37 in LNCaP and 22Rv1 cells. Up (upregulated genes); Down (downregulated genes). C, CSN5 regulated targets in E2F and cell cycle pathways were validated in LNCaP, C4-2, and 22Rv1 cells. D, AR, AR-V7, and FKBP5 expression were detected in shCSN5 (sh37)-treated LNCaP and 22Rv1 cells. E and F, Apoptosis detected by Annexin V assays and immunoblots in LNCaP and 22Rv1 cells. G, Targets of p53 signaling and apoptosis pathway were validated in LNCaP, C4-2, and 22Rv1 cells. H, MYC, FOXM1, CTNNB1, and AURORA protein expression regulated by CSN5. I and J, Four oncogenic pathways enrichment in shCSN5 down-regulated gene group in LNCaP and 22Rv1 cells (I). Some targets of four oncogenic pathways were validated by qRT-PCR (J). K, The correlation of 36 commonly down-regulated genes in three AR (+) prostate cancer cells with metastasis tumor in three prostate cancer cohorts. **, $P < 0.01$; ***, $P < 0.001$; vs. control groups treated with nonspecific (shNS) shRNA.

Figure S4. Knockdown of CSN5 inhibited oncogenic activity of CSN5 in AR-negative prostate cancer cells. A, Four oncogenic pathways enriched in shCSN5 downregulated gene group in CSN5 knockdown PC3 cells. B, 186 prostate cancer SRGs enriched in CSN5 knockdown C4-2 and LNCaP cells. C, The correlation of the 74-gene signature with metastasis in the MSKCC, Grasso, and Yu prostate cancer cohorts.

Figure S5. CSN5i-3 induced antitumor phenotypes in prostate cancer cells. A, Regulation of cullin-RING E3 ubiquitin ligase (CRL) substrates and substrate receptor modules (SRMs) by CSN5i-3. Cells were treated with CSN5i-3 (LNCaP: 5μM; C4-2: 1μM; PC3: 10μM) for 2 days and protein was collected for analysis. B, GSEA of cell cycle and E2F_targets pathways in CSN5i-3 treated LNCaP and 22Rv1 cells. C, Targets of cell cycle and E2F_targets pathways validation in three cell lines by qRT-PCR. D, p53 signaling and apoptosis pathways enrichment in LNCaP and 22Rv1 cells (5μM CSN5i-3). Apoptosis marker was detected by immunoblots. E, Targets of p53/apoptosis pathways were detected in three CSN5i-3-treated prostate cancer cell lines. F and G, Four oncogenic pathways enriched in LNCaP, C4-2, and 22Rv1 prostate cancer cells. GSEA was applied to analyze four oncogenic pathways enriched in CSN5i-3 treated cells (F). Targets of these pathways were detected by qRT-PCR (G). H, The regulation of EMT markers by CSN5i-3 in PC3. I, Phosphokinase array analysis of CSN5i-3-treated C4-2 cells. Each membrane contains kinase-specific antibodies (number indicated). J, Phosphokinase protein expression was validated in CSN5i-3-treated C4-2 cells. Figure values represent the mean ± SE of three independent experiments. *, $P < 0.05$; **, $P < 0.01$; ***, $P < 0.001$; vs. control groups (NC) treated with DMSO.

Figure S6. Synergy between CSN5i-3 and PARPis and transcription cofactor activity of CSN5. A, Spearman's rank correlation matrix of genomic alterations of CSN5 and DNA repair genes in TCGA and SU2C/PCF cohorts. B, Synergy effects of CSN5i-3 and PARPis in PC3 cells. C and D, Synergy effects of CSN5i-3 and olaparib in C4-2 cells. E, The effects on DNA repair gene expression by CSN5i-3 treatment in PC3 and C4-2 cells. Gene expression was detected after 2 days of treatment with CSN5i-3 in PC3 (10μM) and C4-2 (1μM). F, Weight of C4-2 xenograft mice with CSN5i-3 treatment or control. G, Intersection of CSN5-binding genes in CUT&Tag with three CSN5 antibodies from Abcam, Genetex, and Santa Cruz in PC3. H and I, Common transcriptionally downregulated pathways by inhibition of CSN5 in PC3. CSN5 targets were identified by integrating CUT&Tag (with three CSN5 antibodies) with RNA-seq datasets from shCSN5 and CSN5i-3 treated PC3 (H). GSEA was used for pathway analysis by using Hallmark and Reactom pathway signature (I). Figure values represent the mean ± SE of three independent experiments. *, $P < 0.05$; **, $P < 0.01$; ***, $P < 0.001$; vs. control groups (NC) treated with DMSO.